

Optimal Nonadditive Quantum Error-Detecting Code

Wen-Tai Yen and Li-Yi Hsu

Department of Physics, Chung Yuan Christian University,

Chungli 32081, Taiwan, Republic of China

(Date textdate; Received textdate; Revised textdate; Accepted textdate; Published textdate)

Abstract

In this paper, we investigate the optimal nonadditive quantum error-detecting codes with distance two. The numerical simulation shows that, with n being 5, 6, 7, 8, 10 and 12, such the n -qubit quantum error-detecting codes with maximal number of codewords can be found. Therein, except the $n=7$ case, the n -vertex loop graphs help find the optimal quantum codes.

Quantum computation, with the use of the quantum mechanical phenomena, is theoretically proved more efficient than classical computation on problems, such as prime factorization and unsorted database search. However, in physical realization, disturbance from environment can cause unavoidable errors in any quantum information processing. To protect the quantum data, the quantum error-correction/detection codes are exploited to defy decoherence. Over the past decade, extensive studies on quantum error-correcting codes have enhanced the feasibility of large-scale quantum computers in the foreseen future. Therein, an important class of quantum error-correction codes are stabilizer codes, which are additive.

Recently, nonadditive quantum codes without stabilizer structure have attracted some attentions [1, 2]. In brief, an $((n, K, d))$ nonadditive code indicates encoding a K -dimension subspace, which is also called codespace, with distance d into n physical qubits. Smolin *et al* originally proposed the $((5, 6, 2))$ nonadditive quantum error-detection codes [3]. Later a unifying approach was presented by Cross *et al* to construct additive and nonadditive codes, called codeword stabilized codes [4]. Yu *et al* proposed the first $((9, 12, 3))$ quantum code [5]. Notably, so far almost nonadditive quantum codes are on the graph-state basis. Some further properties of codeword stabilized codes were investigated by Chuang *et al* [6, 7]. Later many graphical quantum codes, binary or non-binary, were proposed [9, 10, 11]. It has also been shown that nonadditive quantum codes can outperform the additive ones in some aspects [12].

In this paper, we focus on the codeword stabilized codes with distance two. Rains proposed the upper bound of K with $d = 2$ [8]: if n is even ($n = 2m$),

$$K \leq 4^{m-1}; \tag{1}$$

otherwise ($n = 2m + 1$),

$$K \leq 4^{m-1} \left(2 - \frac{1}{m}\right).$$

In this paper, we numerically verify that some n -qubit nonadditive codeword stabilized codes with $n = 5, 6, 7, 8, 10$ and 12 , respectively, can reach the upper bounds. Before proceeding further, we review codeword stabilizer codes. In brief, an $((n, K))$ codeword stabilizer code can be described on the basis of a specific n -qubit graph state with the associated undirected graph $\mathcal{G}_{c_1} = (V, E)$, $|V| = n$. Denote the neighboring vertex set of the vertex i as $N(i) = \{j | (i, j) \in E\}$. The $n \times n$ symmetric adjacency matrix with vanishing diagonal entries is denoted by Γ and the entry $\Gamma_{ij} = 1$ if $(i, j) \in E$ and 0 otherwise. The

graph state associated with the graph \mathcal{G}_{c_1} reads

$$|c_1\rangle = \prod_{(i,j)\in E} \mathcal{Z}_{ij} |+\rangle^{\otimes n},$$

where \mathcal{Z}_{ij} is the controlled-phase operation between qubits i and j . The corresponding density matrix can be expressed as

$$\rho_{c_1} = \frac{1}{2^n} \prod_{i=1}^n (\mathbf{I} + g_i), \quad (2)$$

where \mathbf{I} is the identity matrix and the stabilizer generator g_i can be written as

$$g_i = X_i \prod_{j\in N(i)} Z_j, \quad i = 1, \dots, n, \quad (3)$$

where X_i and Z_j are Pauli matrices σ_x and σ_z on the qubit i and j , respectively. It is noteworthy that

$$\{Z_i, g_i\} = 0 \quad (4)$$

The codespace of the optimal quantum error-detection code, denoted by \mathfrak{C}_Q , with distance two are spanned by the orthonormal state set $\mathcal{C}_{set} = \{|c_L\rangle | L = 1, \dots, K_{\max}\}$, where

$$|c_L\rangle = \prod_{j=1}^n Z_j^{b_{Lj}} |c_1\rangle, \quad b_{Lj} \in \{0, 1\}, \quad (5)$$

where K_{\max} is equal to 2^{n-2} or $\lfloor 2^{n-2}(1 - \frac{1}{n-1}) \rfloor$ if n is even or odd, respectively. The density matrix of $|c_L\rangle$, ρ_{c_L} , is

$$\prod_{j=1}^n Z_j^{b_{Lj}} \rho_{c_1} Z_j^{b_{Lj}} = \frac{1}{2^n} \prod_{j=1}^n (\mathbf{I} + (-1)^{b_{Lj}} g_j). \quad (6)$$

In this paper, we character $|c_L\rangle$ by the eigenvalues of operators g_1, g_2, \dots, g_n . That is, the n -bit string c_L are expressed as

$$b_{L_1} b_{L_2} \cdots b_{L_n}, \quad (7)$$

since, as according to Eq. (6), the eigenvalue of the g_j the eigenstate $|c_L\rangle$ is b_{L_j} ($c_1 = 0^{\otimes n}$).

The essential advantage of codeword stabilized codes lies on its correspondence to a classical error-correction/detection code with a specific error model. To see this, in the corresponding classical code of \mathfrak{C}_Q , denoted by \mathfrak{C}_C , the n -bit codeword set is $\mathcal{C}_{classical} = \{c_L | L = 1, \dots, K_{\max}\}$. The codeword state $|c_L\rangle$ corresponds the n -bit codeword c_L . Now let $|\bar{c}_L^i\rangle = Z_i |c_L\rangle$. According to Eqns. (6) and (7), $\bar{c}_L^i = b_{L_1} b_{L_2} \cdots b_{L_{i-1}} \bar{b}_{L_i} b_{L_{i+1}} \cdots b_{L_n}$. That is,

in the quantum codespace, the phase-flip error on qubit i corresponds to the bit-flip error on bit i in the classical codespace. Furthermore, according to Eq. (3), it is obvious to verify that

$$X_i |c_L\rangle = \prod_{j \in N(i)} Z_j |c_L\rangle \quad (8)$$

The bit-flip error on the i -th qubit corresponds the multi-qubit phase-flip errors on the neighboring qubits in the quantum codespace. As a result, all single-qubit errors can be regards to only phase-flip errors, which corresponds bit-flip errors on one or more bits in the corresponding classical error model.

In details, the phase-flip error Z_i corresponding bit-flip on the i -th bit. (In the following, by $\overline{1}_k$, we denote n -bit string, where k -th bit is 1 and the other $n - 1$ bits are zeros.) In addition, according to Eq. (8), the single-qubit bit-flip error X_i corresponds to classical $|N(i)|$ bit-flip errors on bits $j_1, \dots, j_{|N(i)|}$, where $(i, j_k) \in E$. As an example, Cross *et al* have originally proposed the optimal $((5, 6, 2))$ codeword stabilized code, where the 5-qubit graph states with 5-vertex cycle (or loop) graph are exploited. Therein, five single-qubit bit-flip errors corresponds to the two-bit-flip classical errors, which are 10100, 01010, 00101, 10010 and 01001, respectively. Finally, the corresponding classical error of single-qubit error Y_i corresponds flipping $(|N(i)| + 1)$ bits $j_1, \dots, j_{|N(i)|}$, and i . In the following, the n -bit strings $\Gamma_{i1}\Gamma_{i2}\cdots\Gamma_{i(i-1)}0\Gamma_{i(i+1)}\cdots\Gamma_{in}$ and $\Gamma_{i1}\Gamma_{i2}\cdots\Gamma_{i(i-1)}1\Gamma_{i(i+1)}\cdots\Gamma_{in}$ by Γ_i^0 and Γ_i^1 , respectively.

Here we define the state set $\mathcal{C}_{i,k}^Q = \{|c_i\rangle, Z_k |c_i\rangle, X_k |c_i\rangle, Y_k |c_i\rangle\}$, where $1 \leq k \leq n$. Obviously,

$$\mathcal{C}_{i,k}^Q \cap \mathcal{C}_{j,k}^Q = \emptyset \quad \forall i \neq j. \quad (9)$$

The corresponding n -bit string set is denoted by $\mathcal{C}_{i,k} = \{c_i, c_{iz} = c_i + \overline{1}_k, c_{ix} = c_i + \Gamma_k^0, c_{iy} = c_i + \Gamma_k^1\}$. Also, $\forall i \neq j, \mathcal{C}_{i,k} \cap \mathcal{C}_{j,k} = \emptyset$.

However, the associated graph of the graph state $|c_1\rangle$ and hence the corresponding error strings Γ_i^0 and Γ_i^1 are unknown. For a given graph \mathcal{G}'_{c_1} as the associated graph of the graph state $|c_1\rangle$, we test whether there is a error-detection code, $\mathcal{C}_{classical}$, with distance two. Here we brief our algorithm as follows.

- (i) Given a \mathcal{G}'_{c_1} and the corresponding error strings $\Gamma_i^{0'}$ and $\Gamma_i^{1'}$ as inputs. Set the value of the variable count as 0.
- (ii) Generate 2^{n-2} n -bit binary strings $s_1, \dots, s_{2^{n-2}}$, ($s_1 = 0^{\otimes n}$) as if $|s_1\rangle, \dots, |s_{2^{n-2}}\rangle$ were

codeword states.

(iii) Define the 2^{n-2} 4-element string set $S_1, \dots, S_{2^{n-2}}$, where $S_i = \{s_i, s_{ix}, s_{iz}, s_{iy}\}$ and $s_{iz} = s_i + \overline{1}_1$, $s_{ix} = s_i + \Gamma_1^{0'}$ and $s_{iy} = s_i + \Gamma_1^{1'}$. Then verify whether the condition

$$S_i \cap S_j = \emptyset, \forall i \neq j \quad (10)$$

is satisfied. If not, go to (ii), else count=count+1 and do (iv).

(iv) Let $c'_1 = 0^{\otimes n}$ and $c'_i \in S_i$ $1 \leq i \leq 2^{n-2}$. Check whether the set \mathcal{C}' ,

$$\mathcal{C}' = \{c'_i | c'_l \neq c'_m + \overline{1}_k \wedge c'_l \neq c'_m + \Gamma_k^{0'} \wedge c'_l \neq c'_m + \Gamma_k^{1'}, \forall k, l, m \text{ and } l \neq m\}, \quad (11)$$

where $1 \leq l, m \leq 2^{n-2}$ and $1 \leq k \leq n$, exists. If yes, $\mathcal{C}' = \mathcal{C}_{classical}$ as the output, else if count $\geq M$ we halt the program, else repeat (ii)-(iv).

In details, in the proposed algorithm, the set S_i generated in (ii) is presumed to be some set $\mathcal{C}_{j,1}$ and hence $c_j \in S_i$ is presumed. To validate the assumption, the Eq. (10) as the necessary condition is tested in (iii). If the assumption is not defied in (iii), in (iv) c'_i is assumed to equal to c_j . If the assumption is validated, there must be some set $\mathcal{C}' = \mathcal{C}_{classical}$. In addition, to generate the string set $S = \{s_i | 1 \leq i \leq 2^{n-2}\}$ in (ii), we random generate $n - 2$ linear-independent n -bit string $x_1, \dots, x_{2^{n-2}}$. Then set S we exploited is $\{\sum_{i=1}^{n-2} \oplus b_i x_i | b_i \in \{0, 1\}\}$. Interestingly, such way of generating S indeed helps find the optimal error-detection codes. Moreover, for a given graph, we halt the program in (iv) after M failures of searching codewords.

Notably, the proposed algorithm is suitable for the even n case, since the upper bound is exactly equal to 2^{n-2} . In this case, $|\mathcal{C}_{classical}| = |S|$ and, as a result, we just verify whether the set \mathcal{C}' validates the condition in Eq. (11). On the other hand, $|S| > |\mathcal{C}_{classical}|$ if n is odd. Therefore, in the odd n case, the algorithm is modified as follows: In (iv), we replace $\{c'_1, c'_2, \dots, c'_{2^{n-2}}\}$ by all of its $\lfloor 2^{n-2}(1 - \frac{1}{n-1}) \rfloor$ -element subset to check whether Eq. (11) is satisfied.

In our simulation, we explore the optimal n -qubit quantum error-detection codes with distance two, where $5 \leq n \leq 12$. Figures (1-6) show the associated graphs of some codeword states with n being 5, 6, 7, 8, 10 and 12, respectively [?]. In addition, it is noteworthy that, except the $n = 7$ case, the loop graphs are exploited to find the optimal quantum error-detection codes with distance two. Finally, lthough a lot of 9- or 11-vertex graphs have been tried, we fail to find the optimal codes.

The author LYH thanks to Dr. I-Ming Tsai for helpful discussion. He also acknowledges support from National Science Council of the Republic of China under Contract No. NSC.96-2112-M-033-007-MY3.

- [1] V.P. Roychowdhury and F. Vatan, arXiv: quant-ph/9710031.
- [2] E.M. Rains, R.H. Hardin, P.W. Shor and N.J.A. Sloane, Phys. Rev. Lett. **79**, 953 (1997).
- [3] J. A. Smolin, G. Smith, S. Wehner, Phys. Rev. Lett. **99**, 130505 (2007).
- [4] A. Cross, G. Smith, J. A. Smolin and B. Zeng, arXiv: 0708.1021.
- [5] S. Yu, Q. Chen, C. H. Lai, C. H. Oh, Phys. Rev. Lett. **101**, 090501 (2008).
- [6] I. L. Chuang, A. W. Cross, G. Smith, J. A. Smolin, B. Zeng, arXiv: 0803.3232.
- [7] X. Chen, B. Zeng, and I. L. Chuang, arXiv: 0808.3086.
- [8] E. M. Rains, IEEE Trans. Info. Theory **45**, 266 (1999).
- [9] S. Yu, Q. Chen, C.H. Oh, arXiv: quant-ph/0709.1780.
- [10] D. Hu, W. Tang, M. Zhao, Q. Chen, S. Yu, C.H. Oh, Phys. Rev. A **78**, 012306 (2008).
- [11] S. Y. Looi, L. Yu, V. Gheorghiu, and R. B. Griffiths, arXiv: 0712.1979.
- [12] Y. Dong, X. Deng, M. Jiang, Q. Chen, S. Yu, arXiv: 0801.1379.

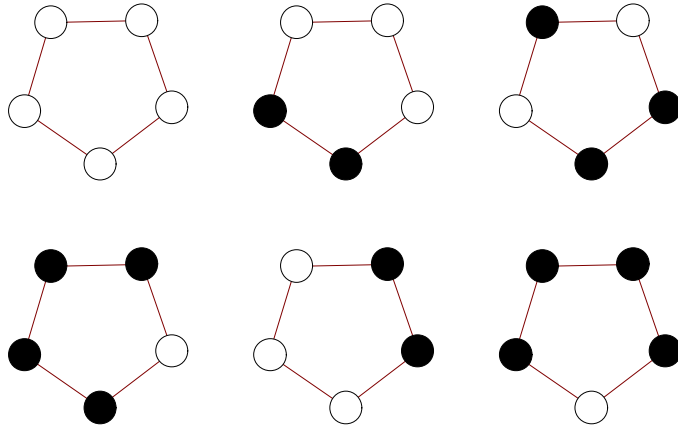


Fig. 1

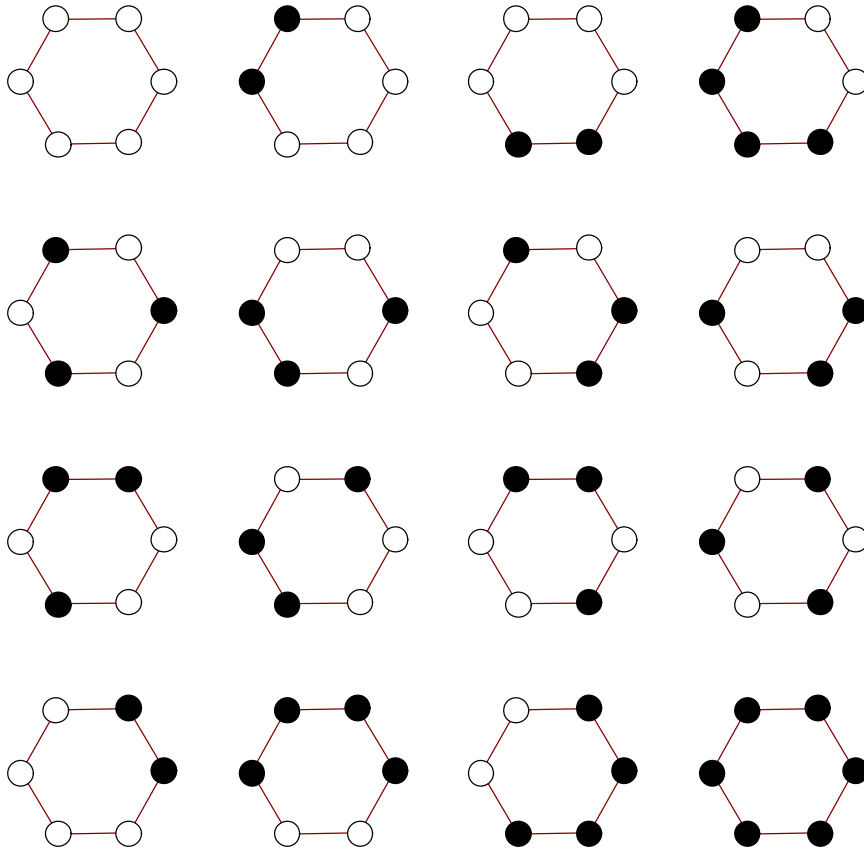


Fig. 2

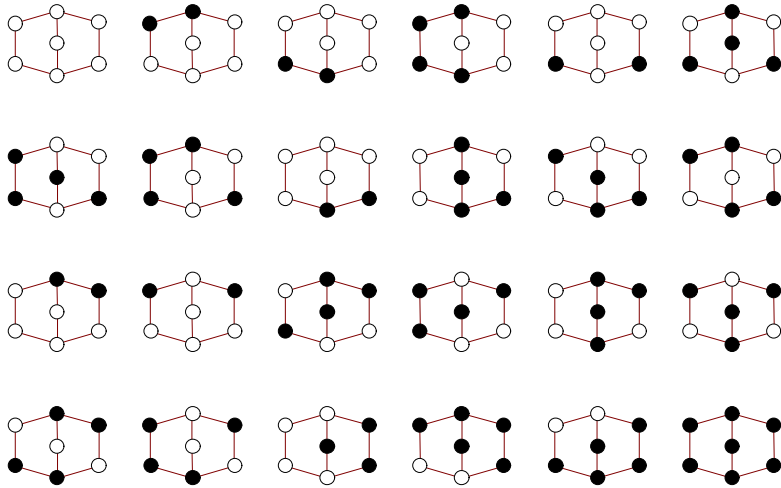


Fig. 3

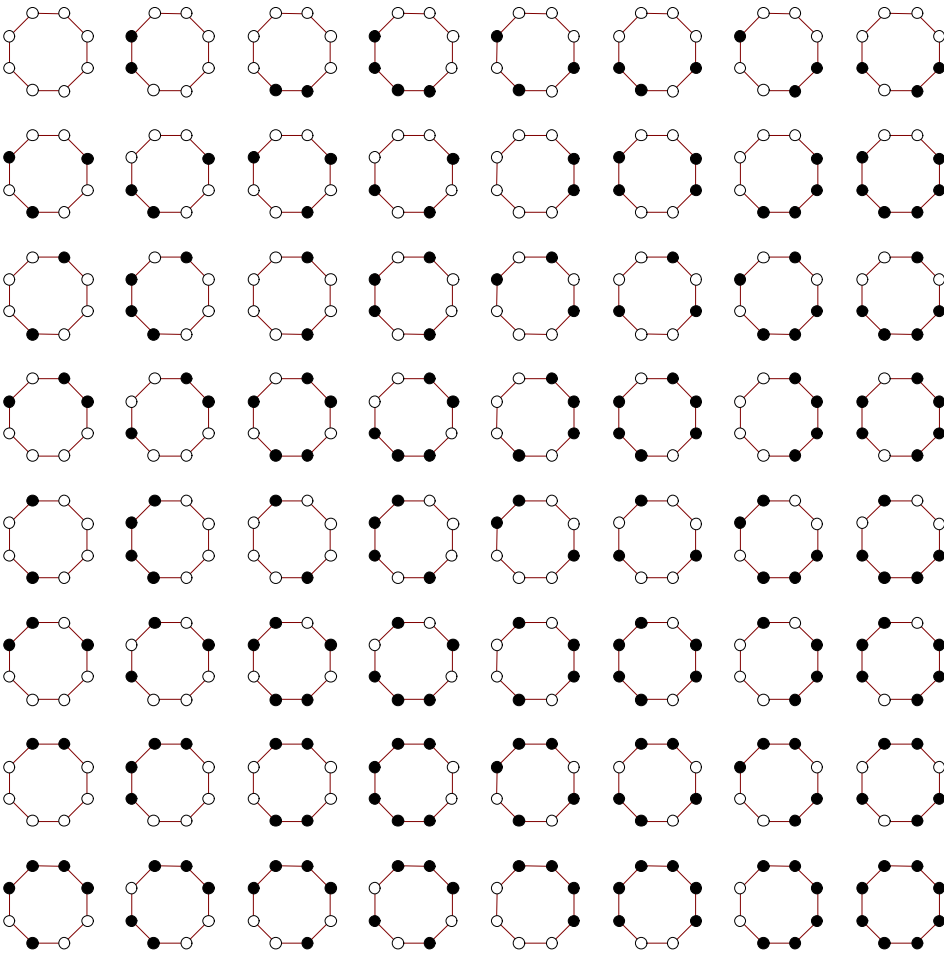


Fig. 4

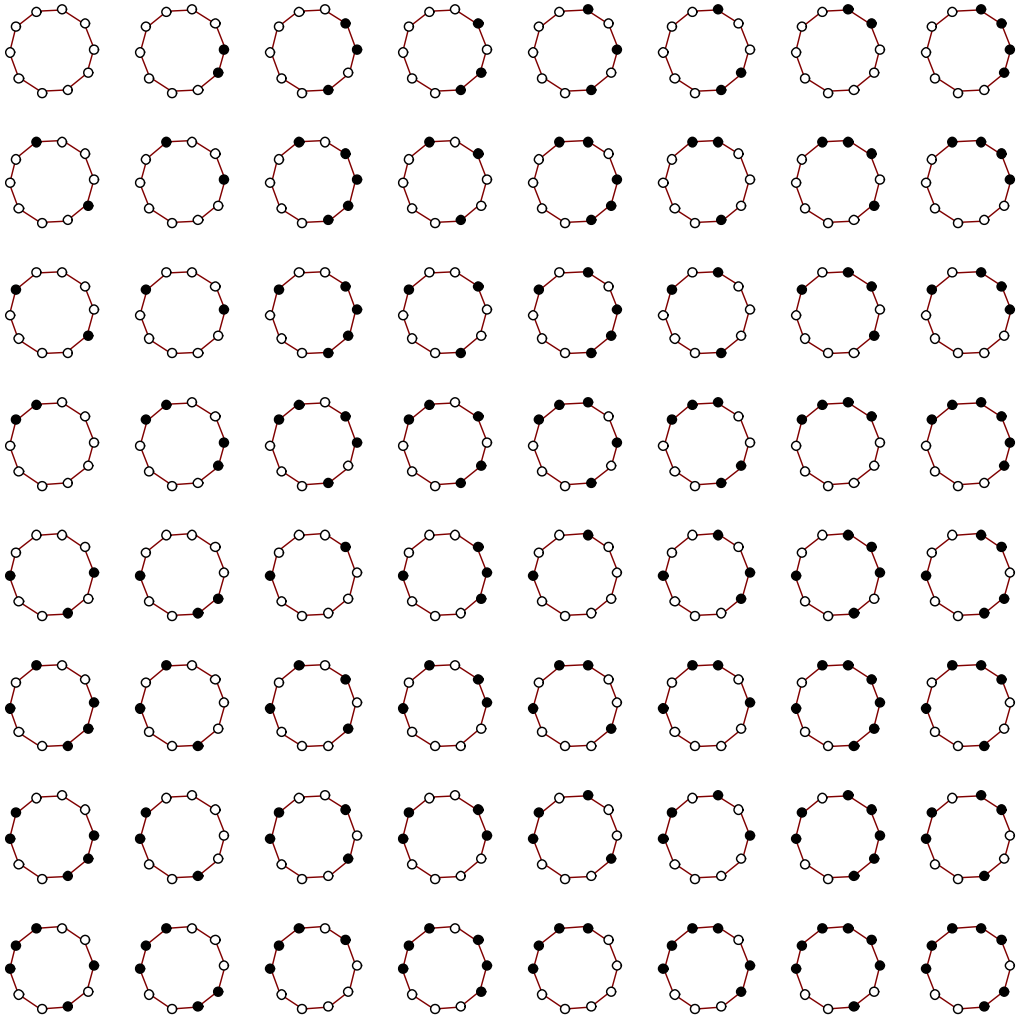


Fig. 5-1

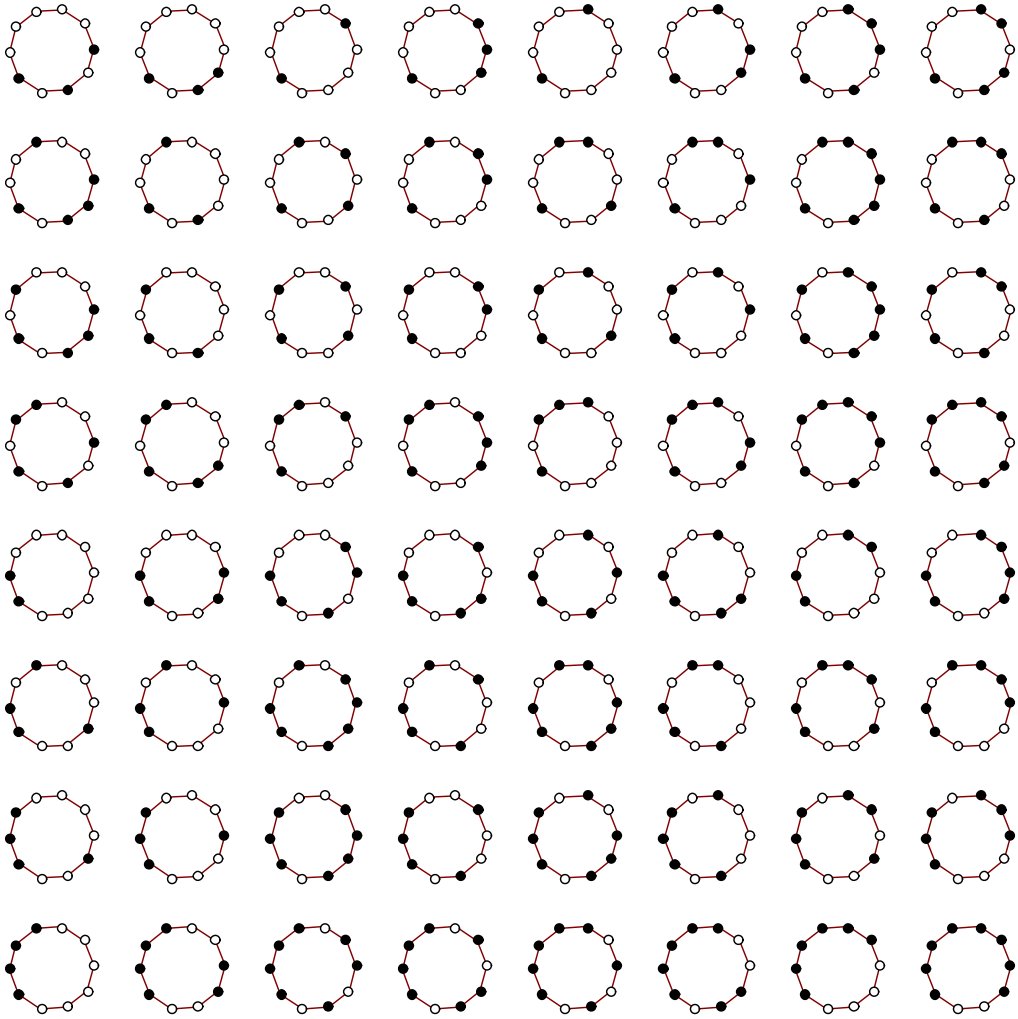


Fig. 5-2

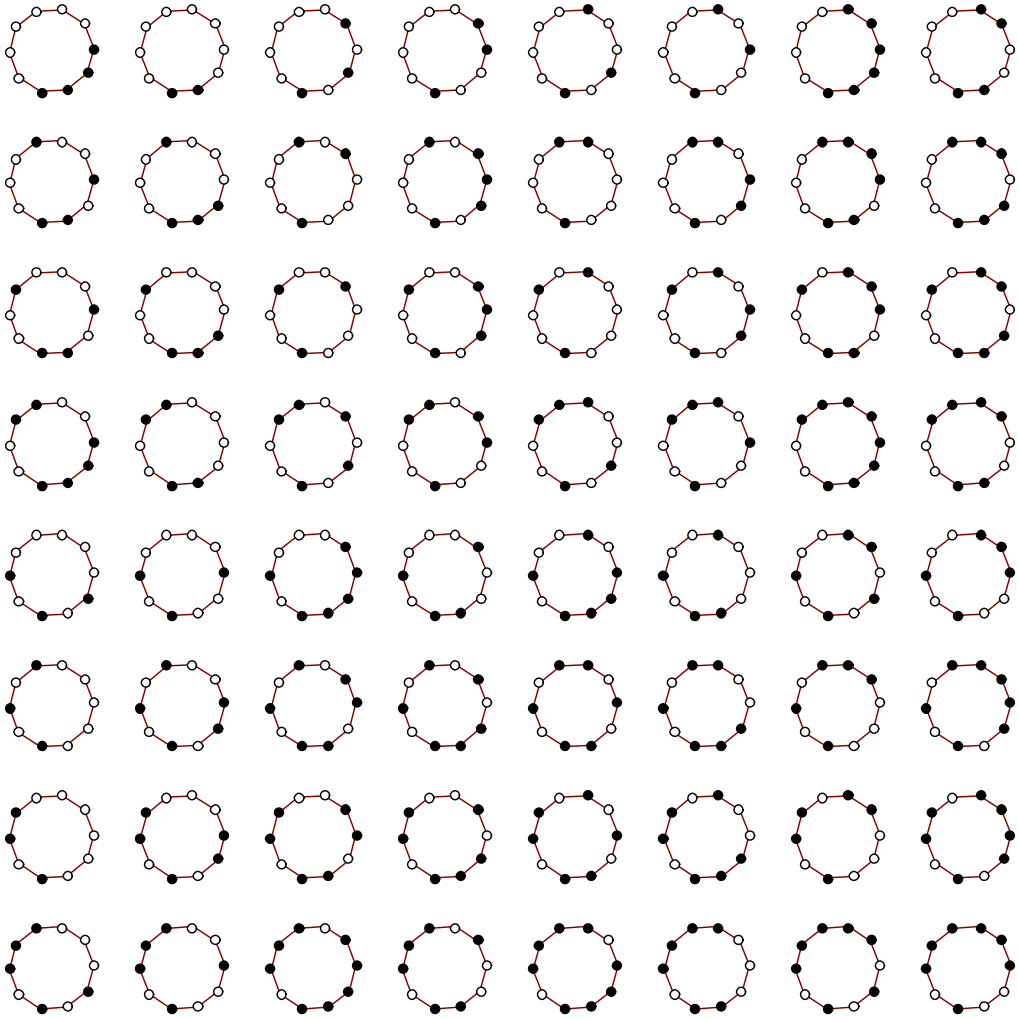


Fig. 5-3

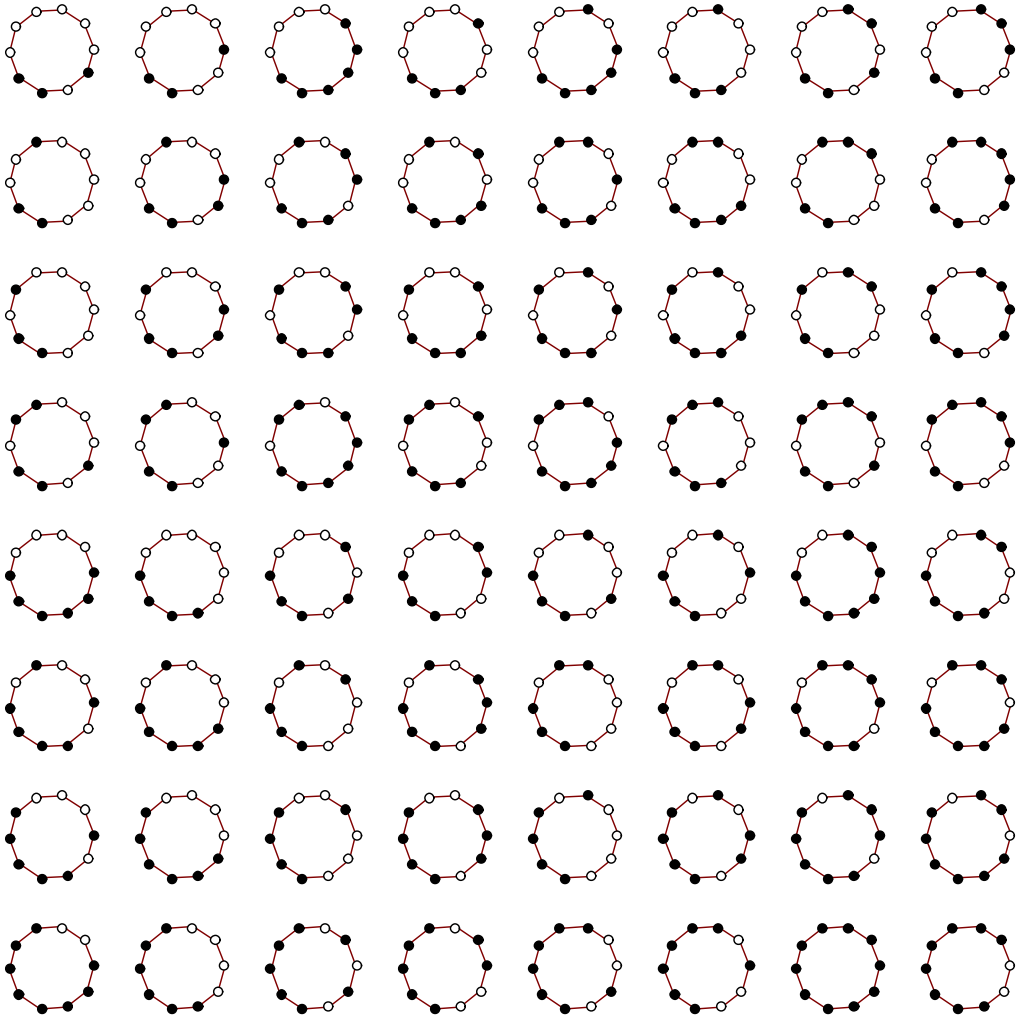


Fig. 5-4

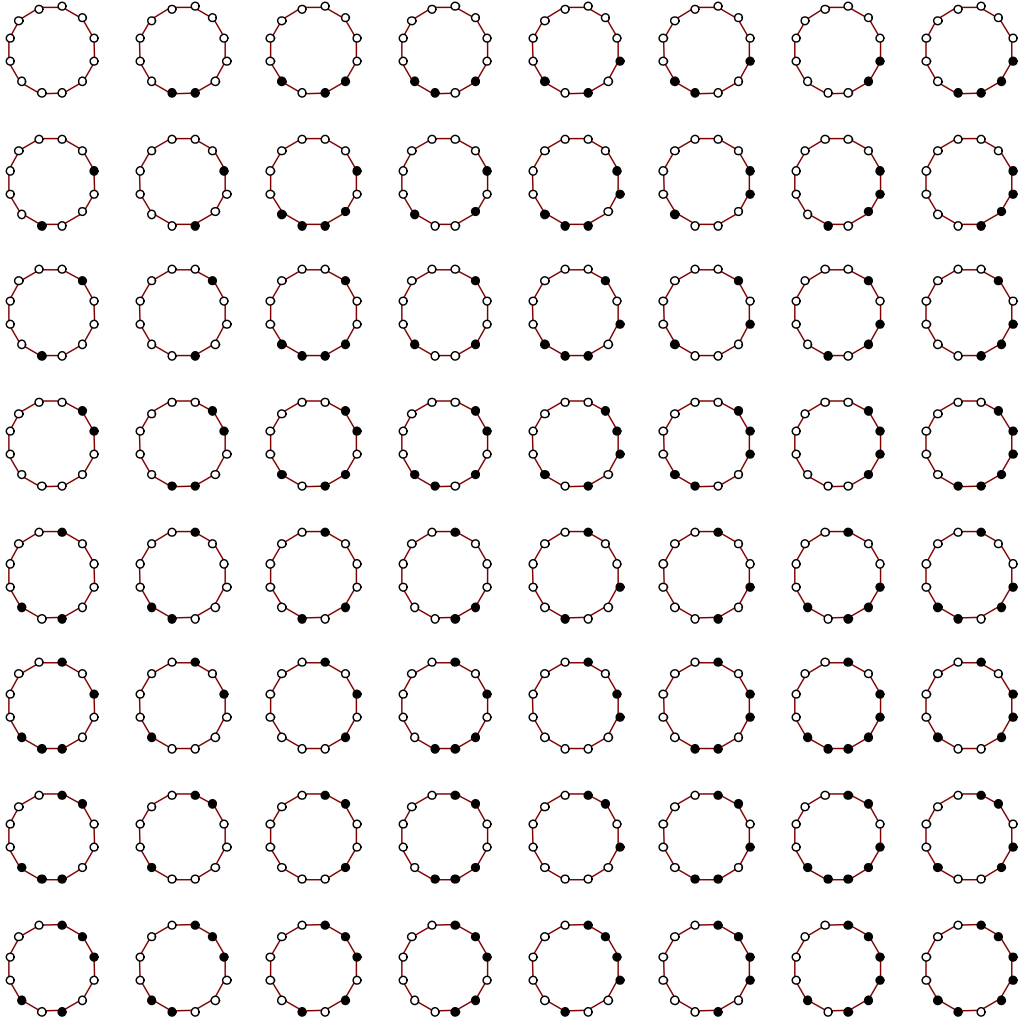


Fig. 6-1

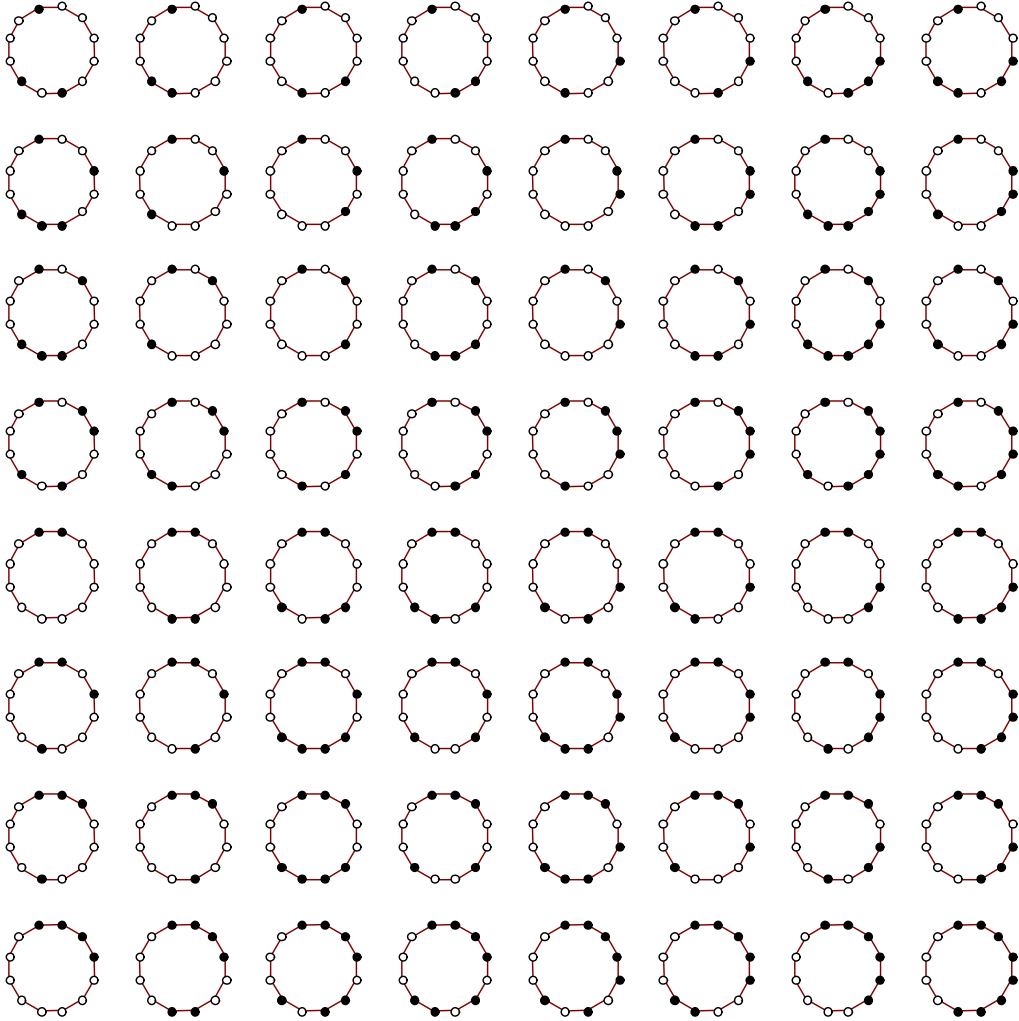


Fig. 6-2

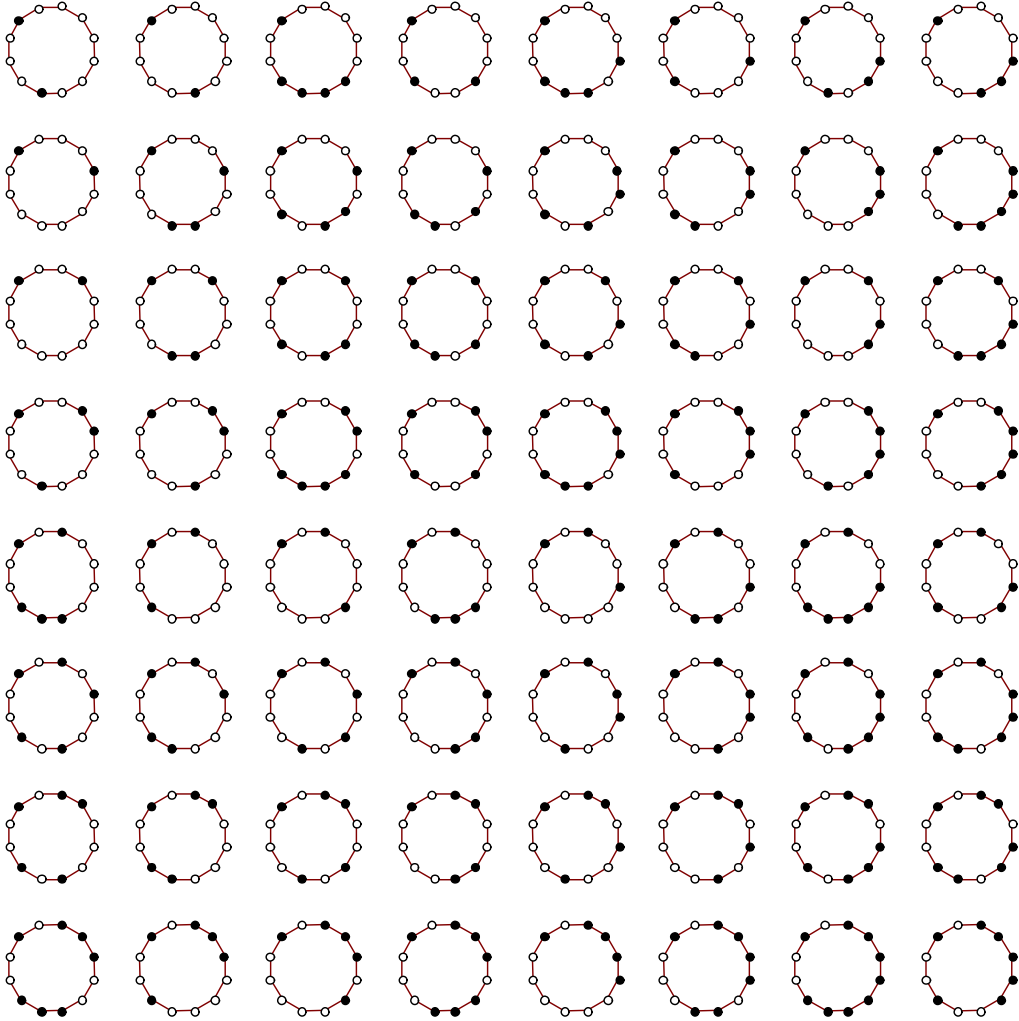


Fig. 6-3

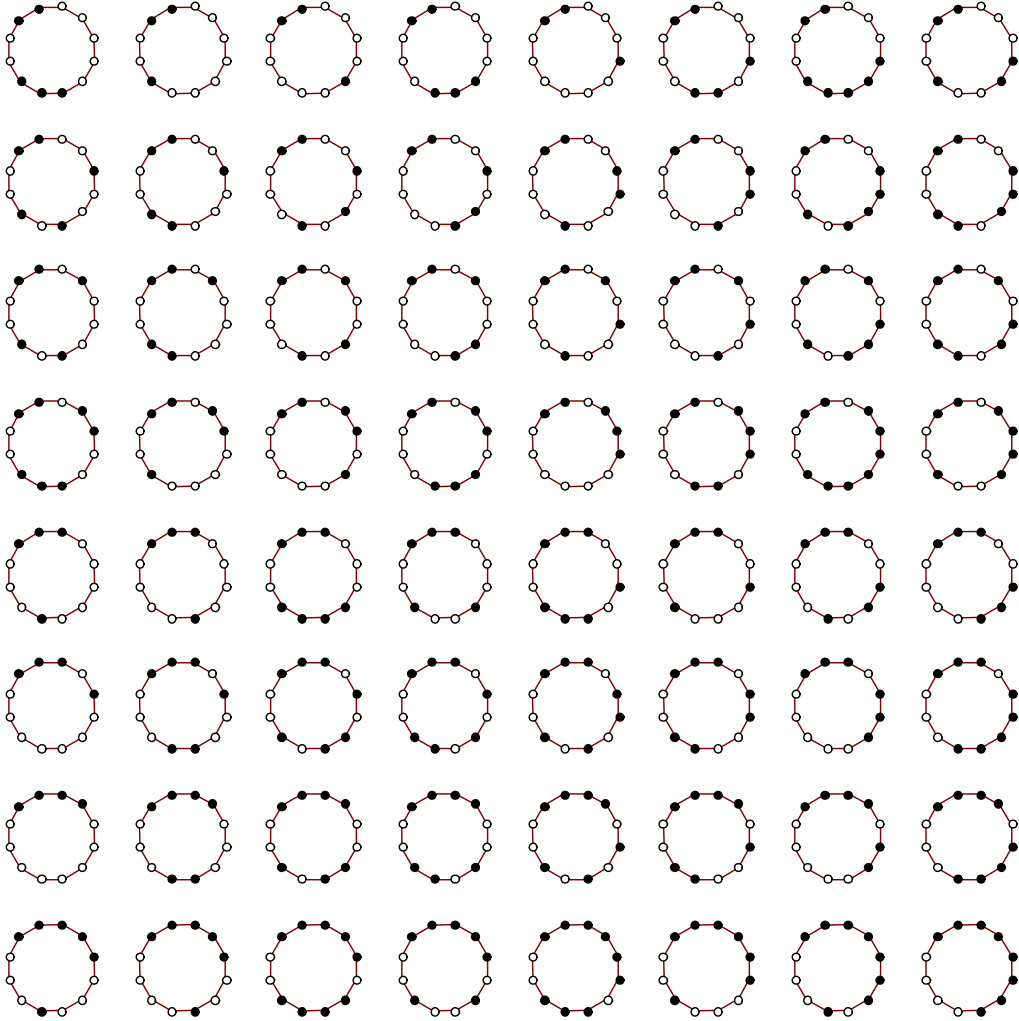


Fig. 6-4

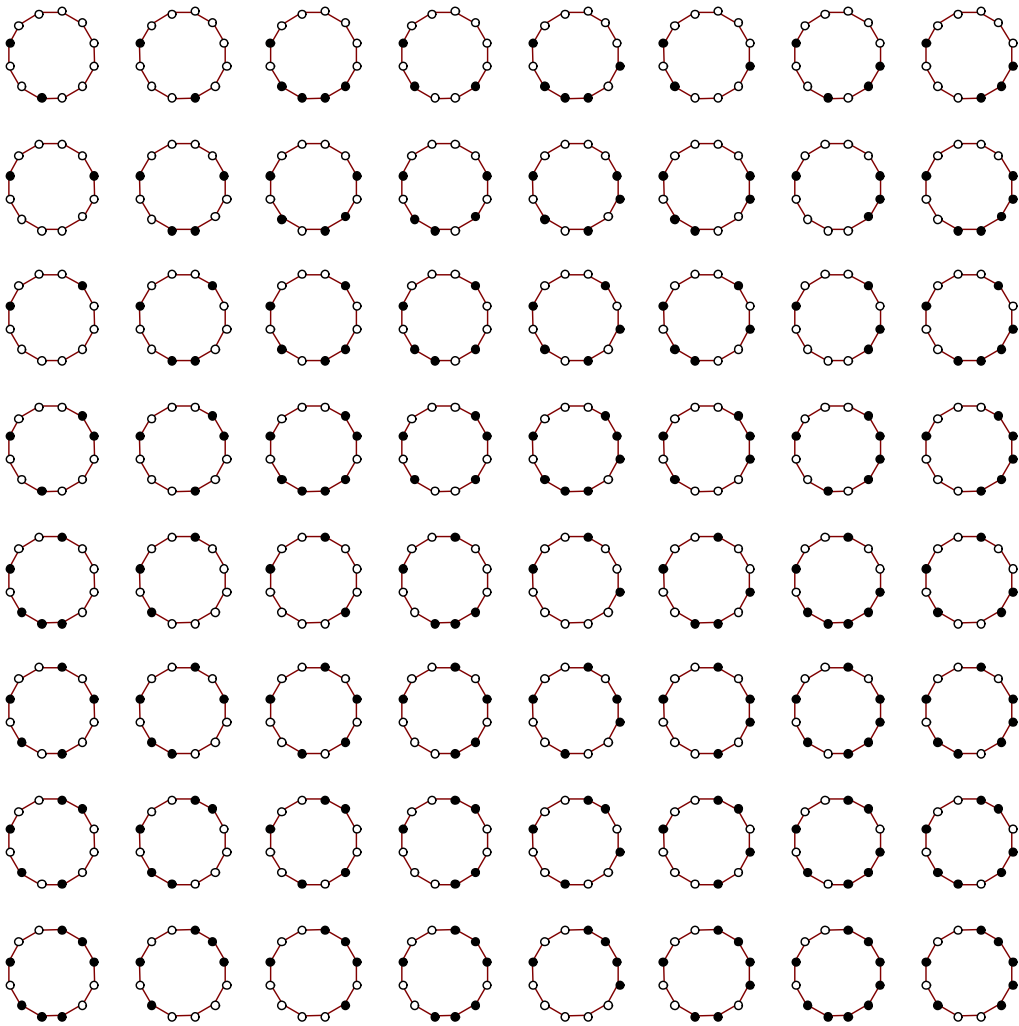


Fig. 6-5

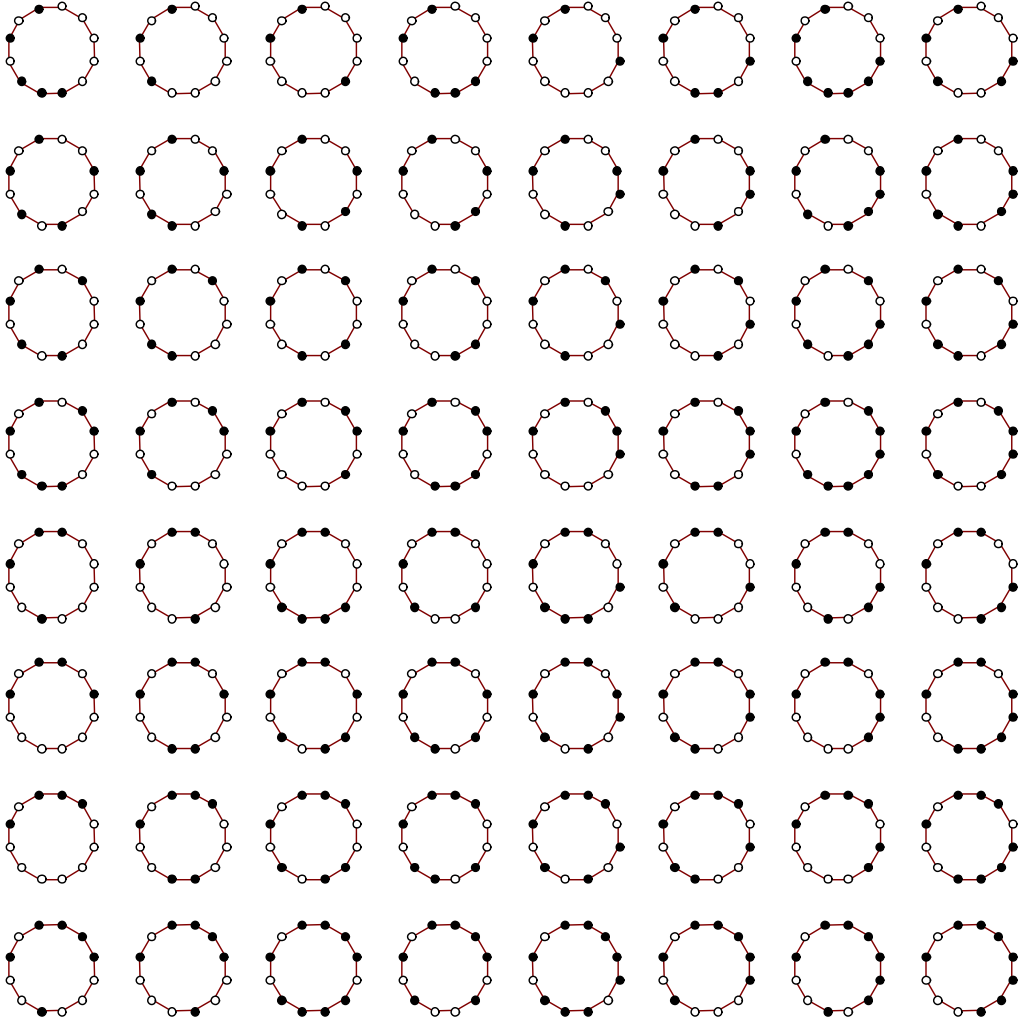


Fig. 6-6

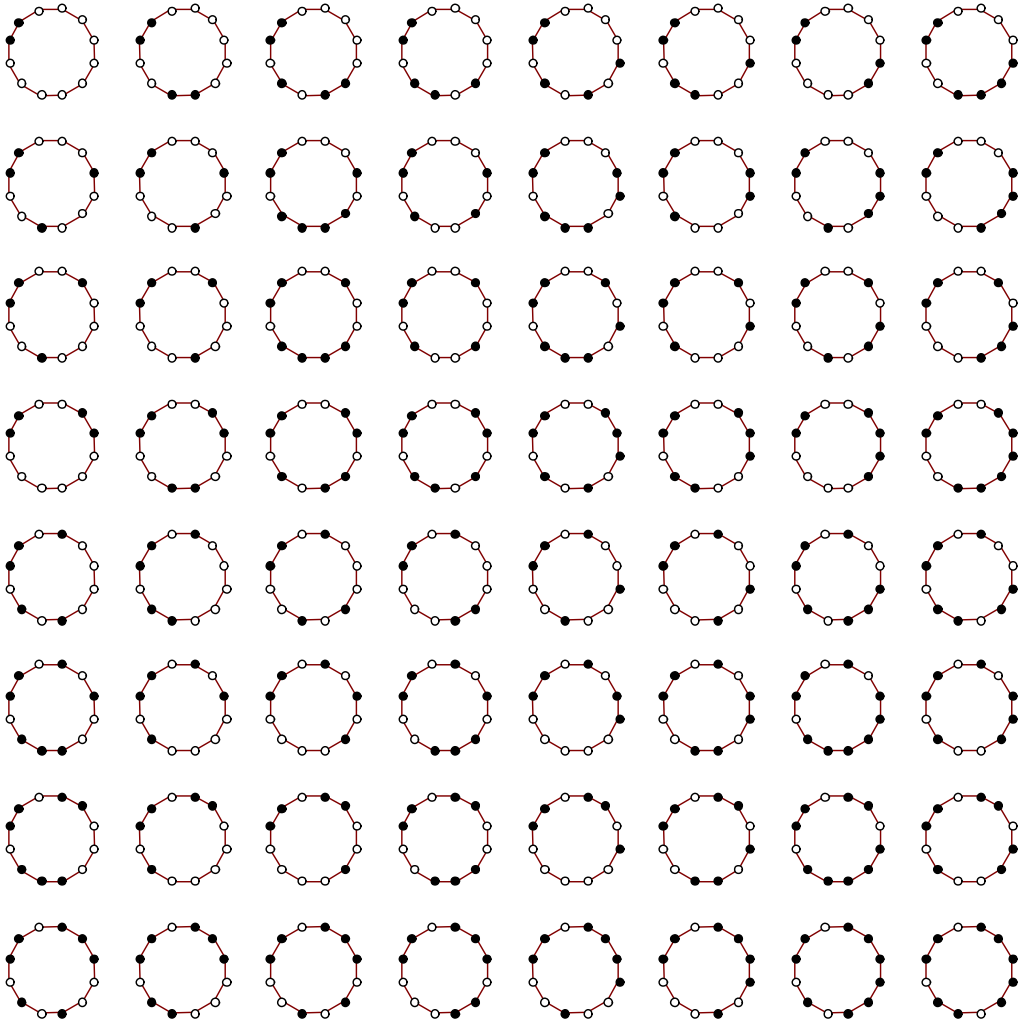


Fig. 6-7

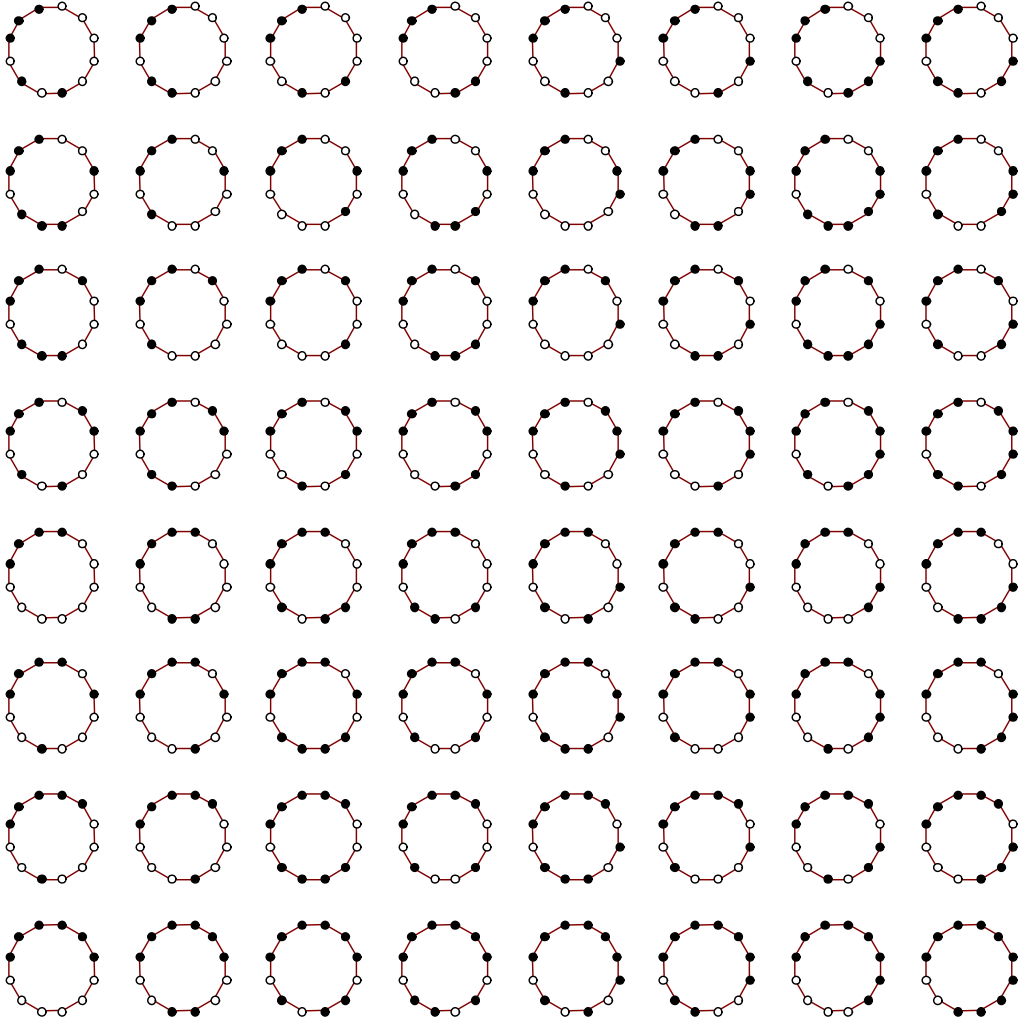


Fig. 6-8

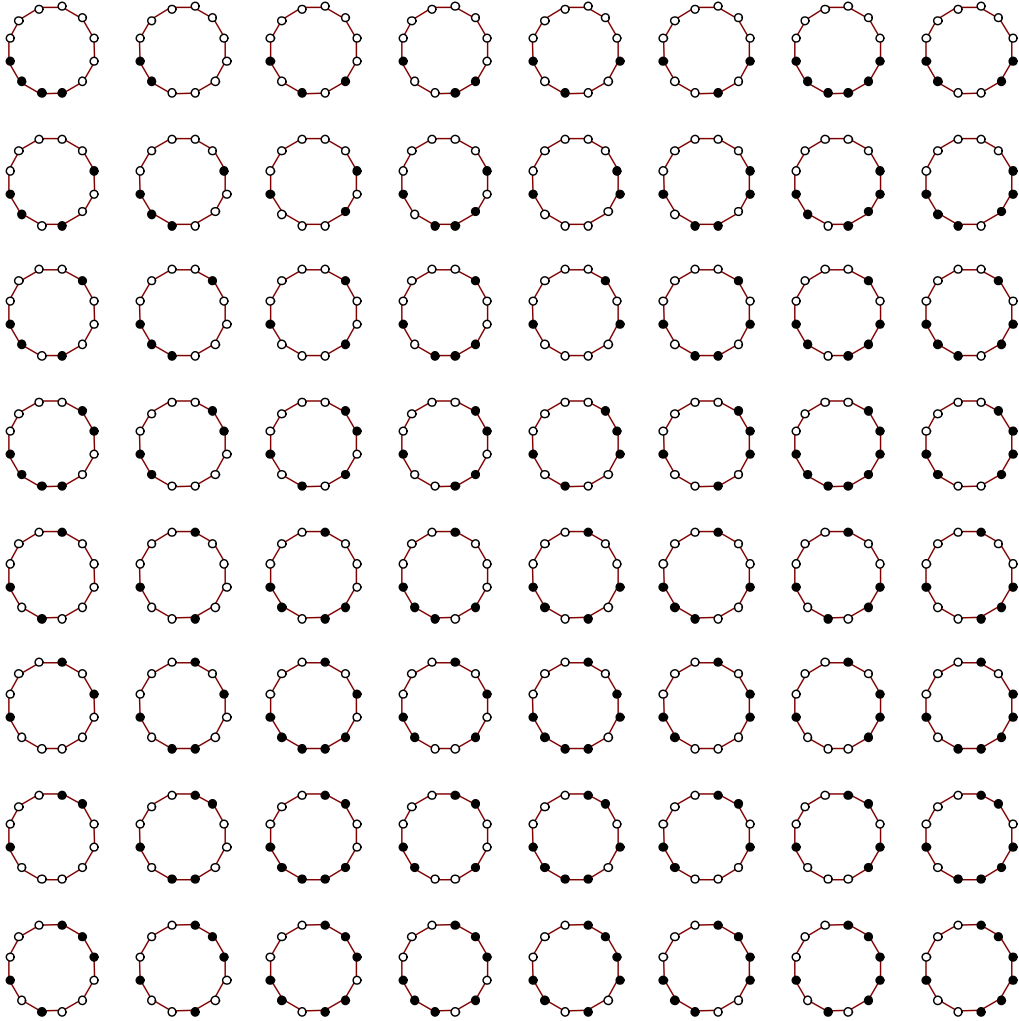


Fig. 6-9

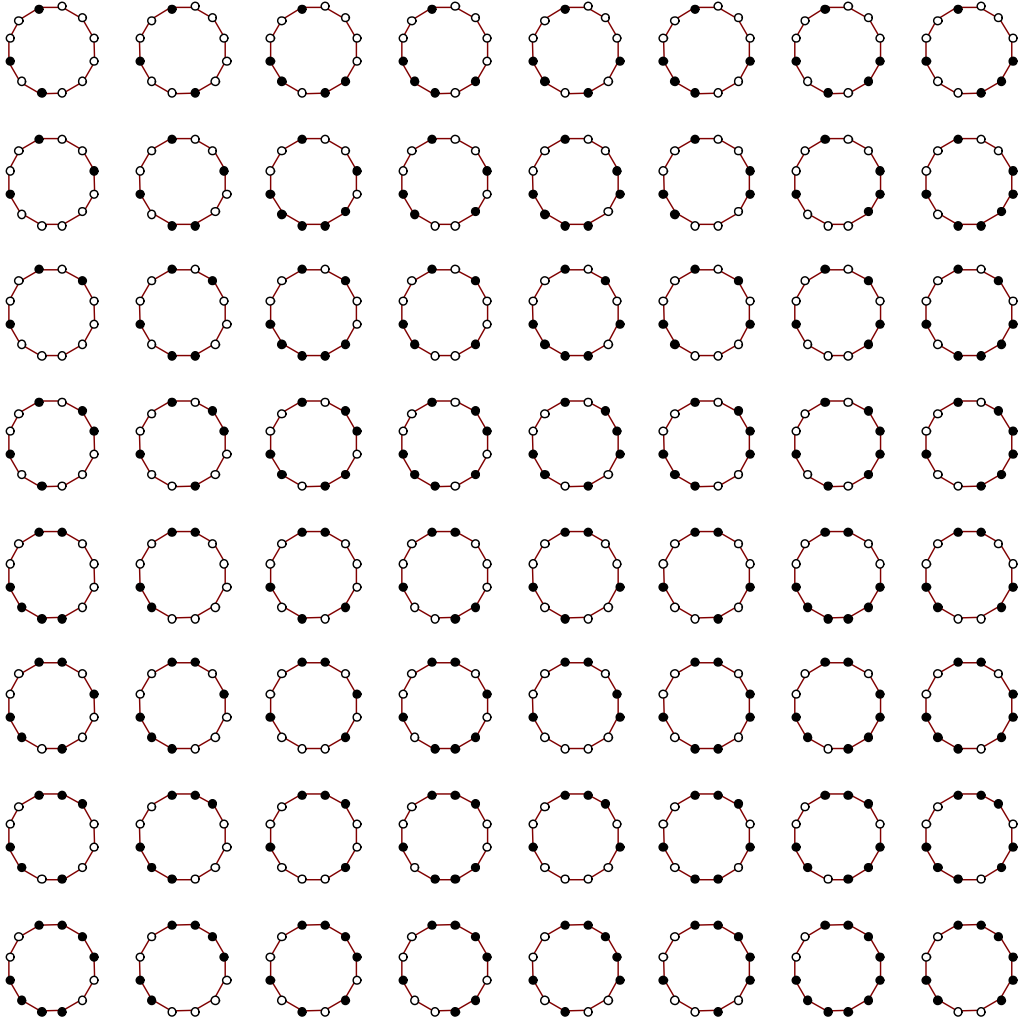


Fig. 6-10

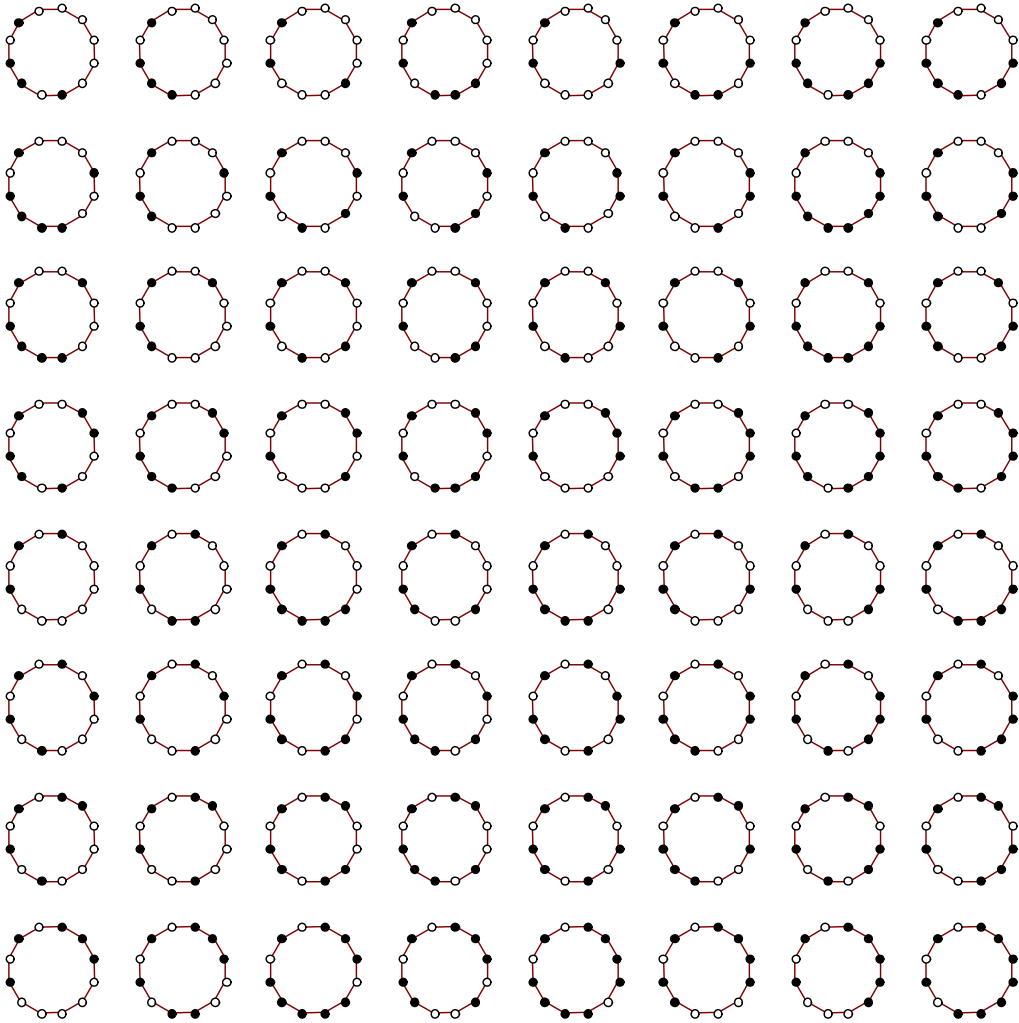


Fig. 6-11

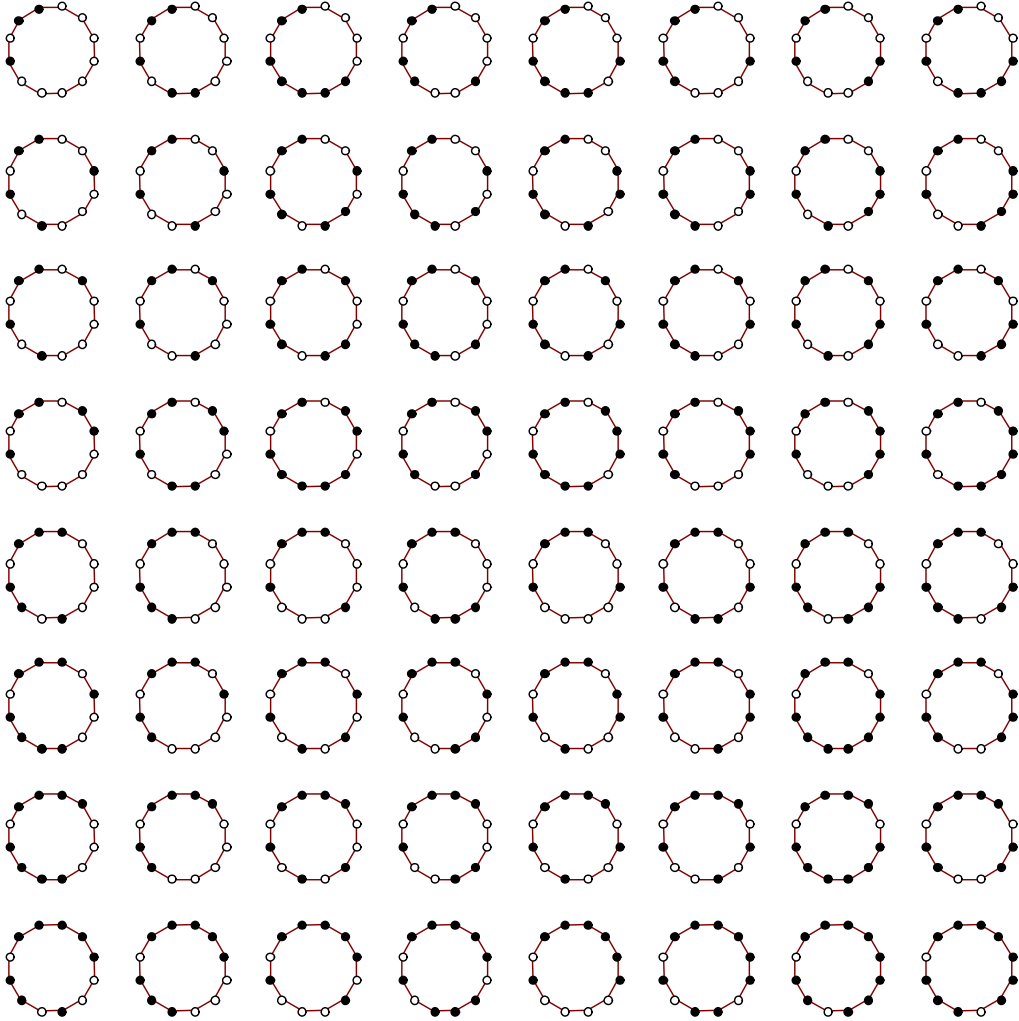


Fig. 6-12

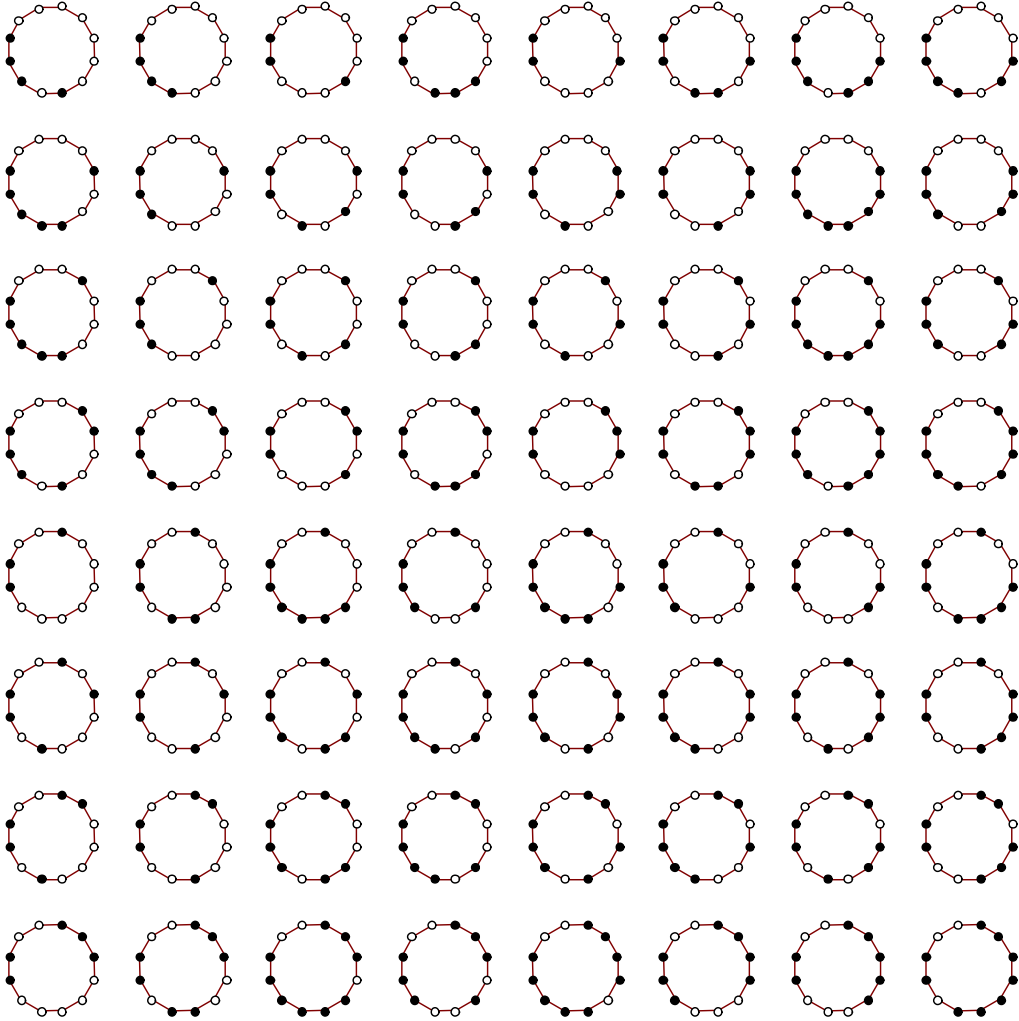


Fig. 6-13

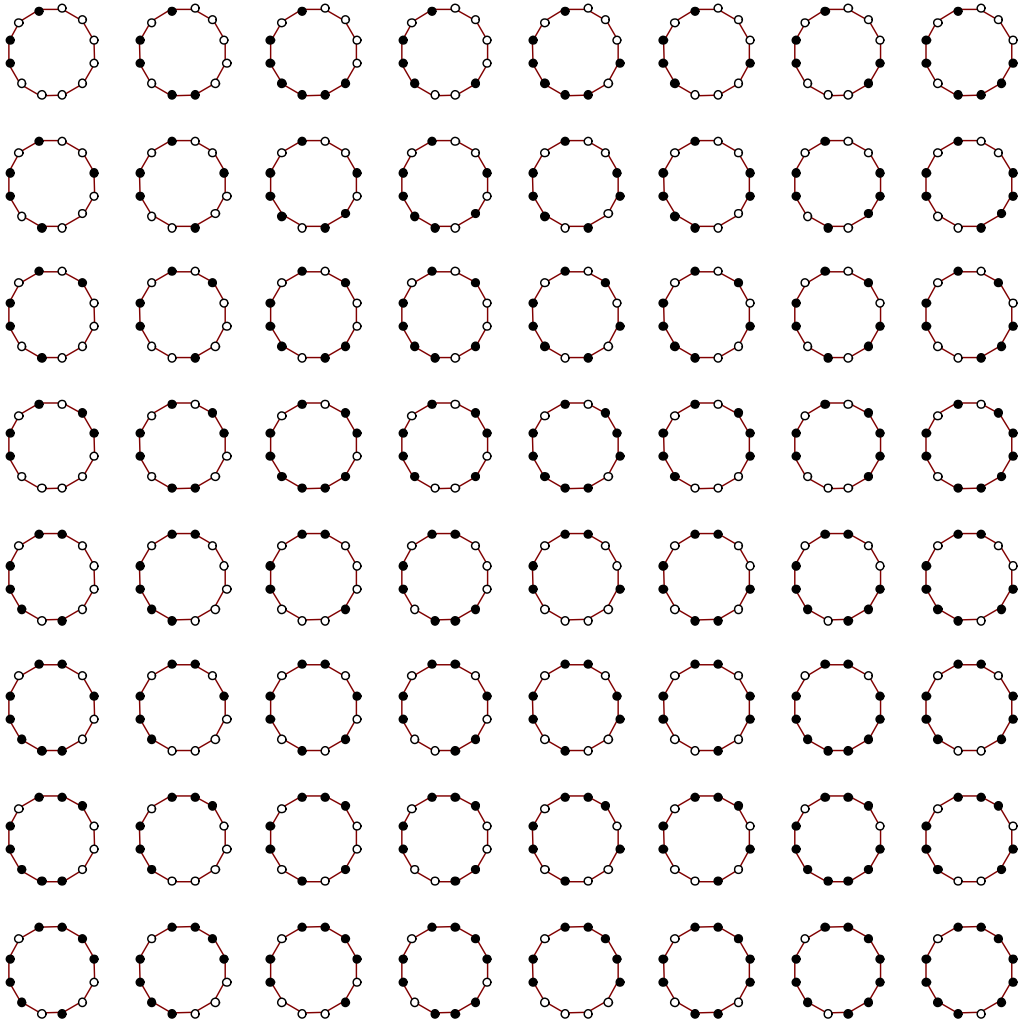


Fig. 6-14

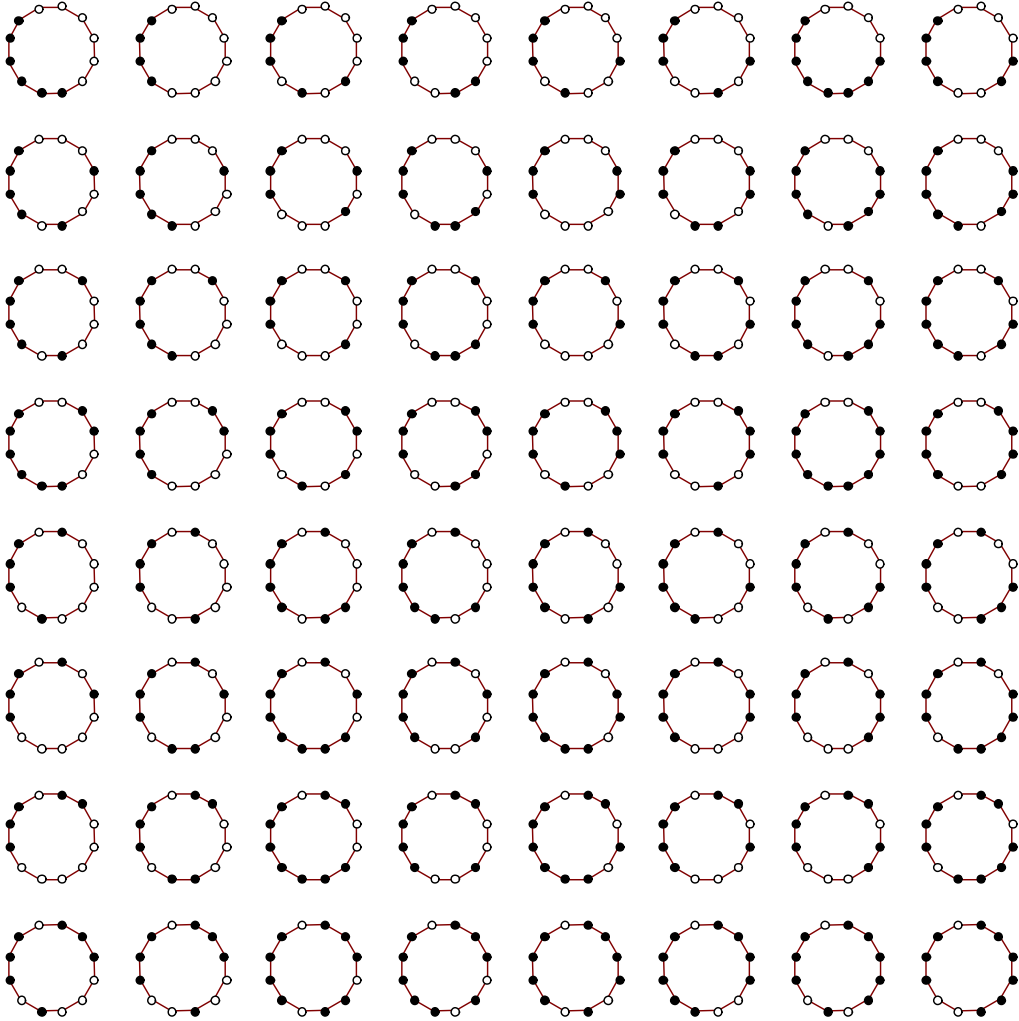


Fig. 6-15

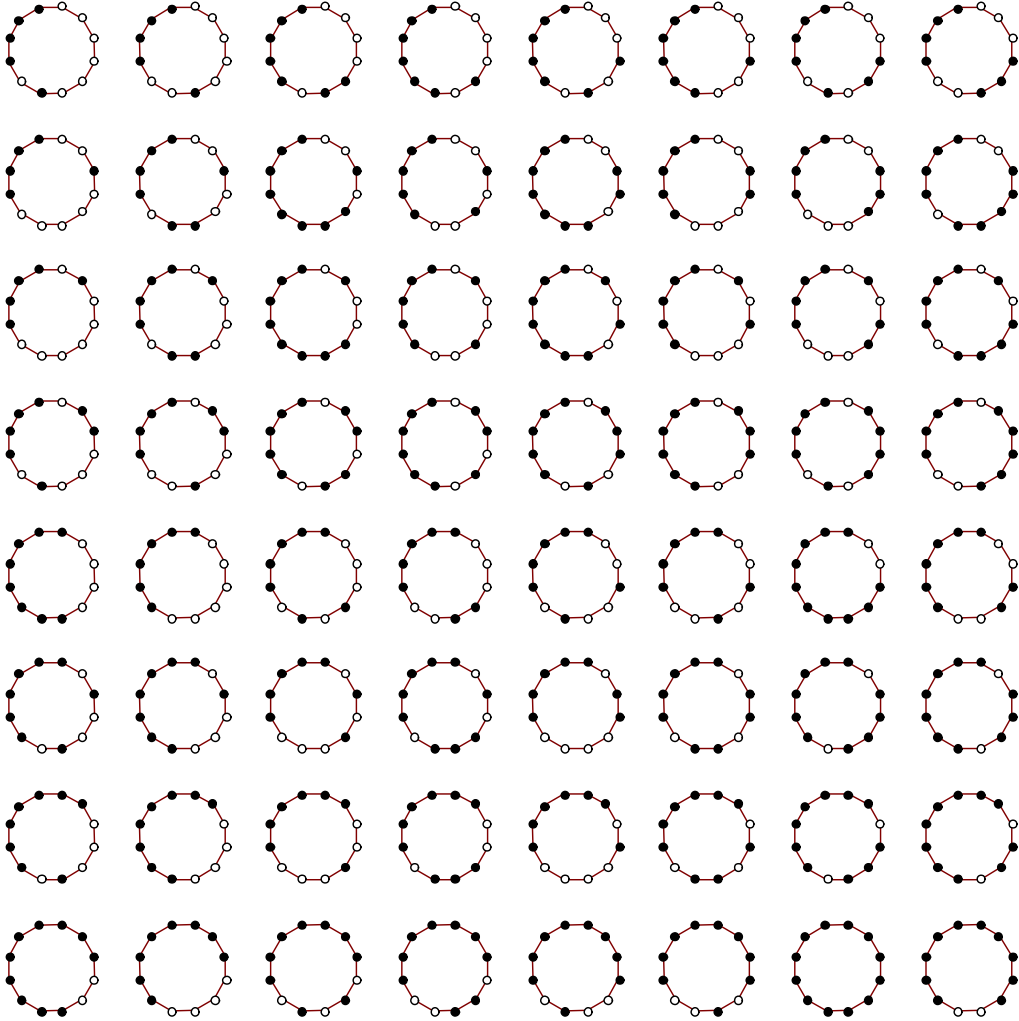


Fig. 6-16